AGU PUBLICATIONS

Water Resources Research

RESEARCH ARTICLE
10.1002/2015WR018326

Flash flooding in small urban watersheds: Storm event hydrologic response

Long Yang[1,2], James A. Smith[1], Mary Lynn Baeck[1], and Yan Zhang[1]

[1]Department of Civil and Environmental Engineering, Princeton University, Princeton, New Jersey, USA, [2]Department of Hydraulic Engineering, Tsinghua University, Beijing, China

Key Points:
- Storm water balance is strongly linked to peak rain rates at time intervals less than 30 min
- Temporal rainfall variability is more important in hydrologic response than its spatial counterpart
- The sensitivity of flood response to spatial rainfall variability is conditioned on storm intensity

Correspondence to:
L. Yang,
longyang@princeton.edu

Citation:
Yang, L., J. A. Smith, M. L. Baeck, and Y. Zhang (2016), Flash flooding in small urban watersheds: Storm event hydrologic response, *Water Resour. Res.*, *52*, 4571–4589, doi:10.1002/2015WR018326.

Received 3 NOV 2015
Accepted 11 MAY 2016
Accepted article online 17 MAY 2016
Published online 18 JUN 2016

Abstract We analyze flash flooding in small urban watersheds, with special focus on the roles of rainfall variability, antecedent soil moisture, and urban storm water management infrastructure in storm event hydrologic response. Our results are based on empirical analyses of high-resolution rainfall and discharge observations over Harry's Brook watershed in Princeton, New Jersey, during 2005–2006, as well as numerical experiments with the Gridded Surface Subsurface Hydrologic Analysis (GSSHA) model. We focus on two subwatersheds of Harry's Brook, a 1.1 km^2 subwatershed which was developed prior to modern storm water management regulations, and a 0.5 km^2 subwatershed with an extensive network of storm water detention ponds. The watershed developed prior to modern storm water regulations is an "end-member" in urban flood response, exhibiting a frequency of flood peaks (with unit discharge exceeding 1 $m^3\ s^{-1}\ km^{-2}$) that is comparable to the "flashiest" watersheds in the conterminous U.S. Observational analyses show that variability in storm event water balance is strongly linked to peak rain rates at time intervals of less than 30 min and only weakly linked to antecedent soil moisture conditions. Peak discharge for both the 1.1 and 0.5 km^2 subwatersheds are strongly correlated with rainfall rate averaged over 1–30 min. Hydrologic modeling analyses indicate that the sensitivity of storm event hydrologic response to spatial rainfall variability decreases with storm intensity. Temporal rainfall variability is relatively more important than spatial rainfall variability in representing urban flood response, especially for extreme storm events.

1. Introduction

In this study, we examine hydrologic response to storm events which led to flash flooding over a small urban watershed, Harry's Brook in Princeton, New Jersey, USA, through combined analyses of rainfall and discharge observations as well as hydrologic modeling experiments. A related study examined the structure and evolution of storms that produced flash flooding over Harry's Brook, and showed that extreme 1–15 min rainfall rates in this watershed are produced by warm season convective systems [*Yang et al.*, 2016]. The question that principally motivates this study is how does rainfall variability together with urban land surface properties (e.g., storm water management infrastructures, storm drainage network, and antecedent soil moisture) determine storm event hydrologic response from flash flood producing storms in small urban watersheds.

Previous observational and modeling studies [e.g., *Ogden et al.*, 2000; *Zhang and Smith*, 2003; *Smith et al.*, 2005a,b, 2013; *Wright et al.*, 2012] showed that spatial-temporal rainfall variability plays an important role in hydrological processes over urban watersheds. This is particularly important for small urban watersheds, which are characterized by short response times, and are consequently very sensitive to rainfall variability [e.g., *Emmanuel et al.*, 2012; *Einfalt et al.*, 2004]. The important role of rainfall variability in urban hydrology has resulted in a large body of research investigating the critical temporal and spatial resolutions of rainfall fields for urban flood response [e.g., *Schilling*, 1991; *Berne et al.*, 2004; *Einfalt et al.*, 2004; *Segond et al.*, 2007; *Gires et al.*, 2012, 2014; *Wang et al.*, 2012; *Notaro et al.*, 2013; *Ochoa-Rodriguez et al.*, 2015; *Bruni et al.*, 2015, among others]. *Ochoa-Rodriguez et al.* [2015] found that variations in temporal resolution of rainfall inputs affect urban hydrodynamic modeling more than variations in spatial resolution. However, *Bruni et al.* [2015] showed that sensitivity to temporal resolution of rainfall inputs was low compared to spatial resolution. Contrasting findings suggest that the sensitivity of hydrologic response to rainfall variability is dependent on storm properties and/or basin characteristics (e.g., spatial scale and heterogeneity). *Hollis* [1975] found

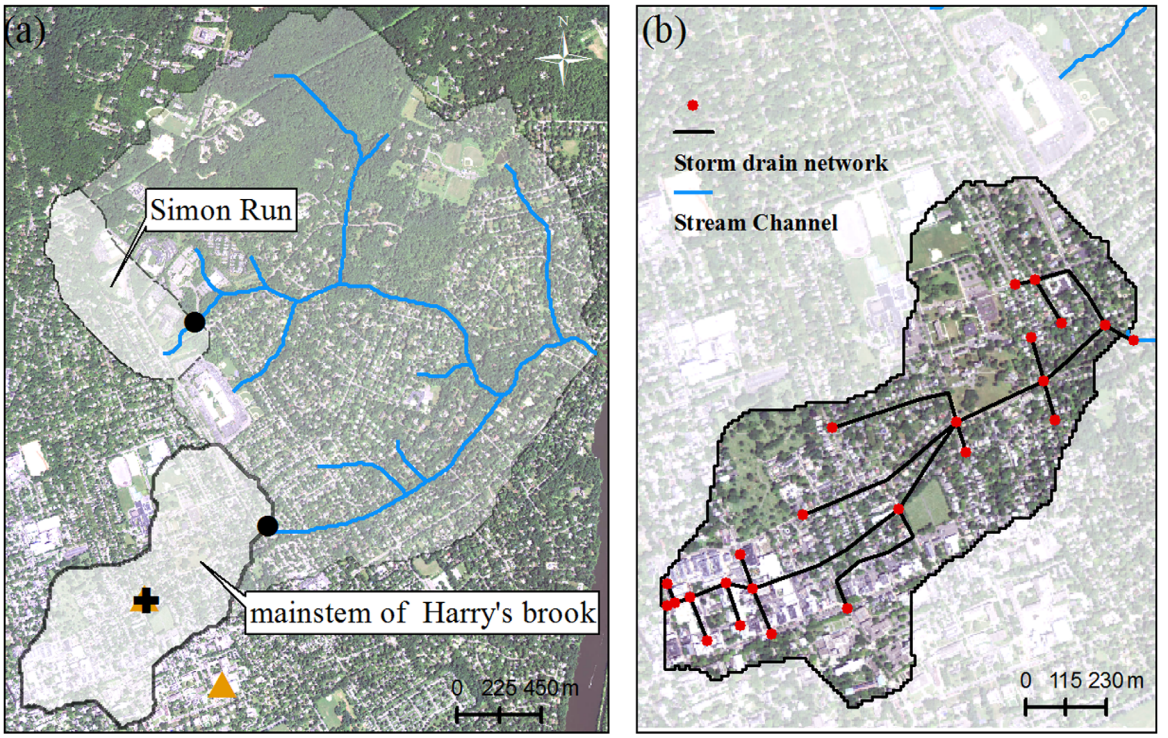

Figure 1. (a) the study watershed, Harry's Brook, covers the shaded grey area with its tributaries shown in blue solid lines. Two subwatersheds (0.5 km^2 Simon Run and 1.1 km^2 Harry's Brook subwatershed) are highlighted as well. Black dots represent stream gaging stations. A Joss-Waldvogel disdrometer is located in the center of the Harry's Brook subwatershed, and is represented by a black cross. Two rainfall measurement sites are represented by yellow triangles; (b) details of the mainstem of Harry's brook subwatershed, including the storm drainage network. The background map is an earth-view image of the entire region (extracted from the USGS national map via http://nationalmap.gov/).

that the impact of urbanization on hydrologic response depends on recurrence levels of floods. Similarly, we hypothesized that storm intensity (represented by accumulated rainfall) is an important factor in determining the relative sensitivity of storm event hydrologic response to rainfall variability. We will test this hypothesis over Harry's Brook, a small urban watershed, based on the examination of a large sample of storm events (14 events, which is larger than storm samples in most previous studies).

The impacts of urban land surface properties on hydrological processes have been active research topics over the last few decades [e.g., *Anderson*, 1968; *Beighley*, 2003; *Hundecha and Bárdossy*, 2004; *Farahmand et al*., 2007; *Smith et al*., 2013; *Yang et al*., 2010, 2013, 2015]. An increase in the fraction of impervious surfaces and introduction of storm drainage systems typically lead to an increase in flood peaks and a decrease in lag time between maximum rainfall rate and peak discharge [e.g., *Leopold*, 1968; *Konrad and Booth*, 2002; *Konrad*, 2003; *Zhang and Shuster*, 2014] (also see *Shuster et al*. [2005] for a review). *Ogden et al*. [2011] evaluated the relative importance of several characteristics (including impervious area, drainage density, width function, and subsurface storm drainage) on urban runoff through numerical experiments using a physically based hydrological model. In addition, the storage over impervious surfaces with microrelief, such as road surfaces constituted from gravel and asphalt and highway embankment, also proved to be an important factor in hydrologic response over urban watersheds [see e.g., *Albrecht*, 1974; *Wibben*, 1976; *Sauer et al*., 1983] (also *Shuster et al*. [2005], for a review). A related aim of this study is to analyze the role of basin characteristics (e.g., storm water management infrastructures, storm drainage network, depression storage, and antecedent soil moisture) in determining storm event hydrologic response. More importantly, we will place these analyses in the context of rainfall variability. *Smith et al*. [2005b] showed that for small urban watersheds in the Baltimore metropolitan region, drainage network structure reduces the role of spatial rainfall variability for flood peak response.

The 6.8 km^2 Harry's Brook watershed (Figure 1) is located in the Piedmont physiographic province of the eastern U.S. and contains portions of Princeton, New Jersey. The watershed has experienced rapid urban and suburban growth since the 1950s, and much of this development predated the introduction of storm

water management regulations in the 1970s. Mixed residential and commercial development since the 1970s in the northwestern portion of the basin (Figure 1) has produced a region with a relatively high density of storm water detention basins. Analyses in this study focus on two subwatersheds of Harry's Brook: (1) Harry's Brook at the intersection of Harrison St and Hamilton Ave, a 1.1 km^2 subwatershed which drains the urban core of Princeton and was entirely developed prior to storm water management, and (2) Simon Run, a 0.5 km^2 subwatershed with an extensive system of storm water detention ponds in the west portion of the Harry's Brook watershed. High-resolution rainfall and runoff records were collected over the two Harry's Brook subwatersheds during a 2 year period (from February 2005 to October 2006). These observations provide the capability to accurately estimate storm total rainfall for basin-scale water balance analyses and characterize rainfall-runoff relationships of flash floods. Differences in storm water management between the two subwatersheds also provide an opportunity to investigate the impacts of urban land surface properties on storm event hydrologic response.

The remaining sections of the paper are organized as follows. Detailed properties of the two subwatersheds are introduced in section 2, along with methods used for streamflow and rainfall monitoring. We introduce the hydrologic model used for examining storm event hydrologic response and numerical experiments in section 3. Results and discussion are presented in section 4, followed by summary and conclusions in section 5.

2. Study Area and Data Sets

2.1. Study Area

Experimental and modeling analyses in Harry's Brook draw on resources developed by the Princeton municipal government, including engineering design drawings of the storm water infrastructure (including the storm drainage system and storm water detention basins) and land use/land cover data sets. The 1.1 km^2 subwatershed that drains the urban core of Princeton is almost exclusively urban land cover based on the USGS land use/land cover data set; we will subsequently refer to this subwatershed as Harry's Brook. The Harry's Brook gaging station is located immediately downstream of the main storm drain outfall that is the upstream end of the surface channel system (Figure 1a). There are no surface channel segments in the watershed above this station. This subwatershed includes high-density commercial and residential development. The impervious coverage accounts for 36.8% of total area of the Harry's Brook subwatershed, with a relatively larger impervious fraction in the upper watershed (downtown Princeton) and a lower impervious fraction in the downstream portion of the subwatershed (principally residential). The mean slope of the watershed is 3.5%. The storm sewer drainage network of Harry's Brook (Figure 1b) was designed to move water efficiently and rapidly from the urban center of Princeton. The density of the storm drainage network in the upper portion of the subwatershed is relatively large, compared to the rest of the subwatershed (Figure 1b).

The 0.5 km^2 Simon Run subwatershed (Figure 1a) contains a mix of residential, commercial, and forest land use, with impervious coverage accounting for 20.1% of the entire watershed. The mean slope of Simon Run is 4.4%. Much of the residential and commercial development was constructed following the introduction of storm water management regulations, resulting in a distributed network of small storm water detention ponds throughout the subwatershed. The contrasts between Simon Run and Harry's Brook are used to examine the role of storm water detention ponds in changing storm event hydrologic response.

2.2. Instrumentation and Data

We deployed stream gaging stations on Harry's Brook and Simon Run. An important element in estimating runoff is developing stage-discharge rating curves, which convert time series of stage (i.e., water surface elevation) to discharge. Stage measurements are made using a pressure transducer, which measures the water level at 1 min interval (Figure 1a). The stage recorders were deployed in straight channel reaches. The Harry's Brook channel is deeply entrenched, due to the discharge of high-flow events from the storm drain network immediately upstream of the gaging station. The observing period for the two stream gaging stations is from February 2005 to October 2006.

Developing accurate discharge estimates for extreme stage values is especially difficult in small urban watersheds, and these values play an important role in water balance analyses. In this study, stage-

Table 1. Structural Properties of Storm Elements That Produced Flash Floods Over Harry's Brook Subwatershed During the Observing Period of 2005–2006

	Spatial Coverage of Storm Elements (km^2)	Storm Speed ($km\ h^{-1}$)	Storm Direction (°)
Mean	161	43	75
Standard deviation	189	11.8	20.5
10th percentile	41	13.8	25
25th percentile	61	31	56
50th percentile	84	42.5	65
75th percentile	157	47.3	97
90th percentile	452	60	101

[a]Adapted from *Yang et al*. [2016, Table 2]. Storm direction of 0° is toward north.

discharge rating curves for each stream gaging station were developed using both direct discharge measurements (with more than ten storm events) and hydraulic modeling analyses. Direct discharge measurements of large urban flood events are difficult due to the inherent hazards and the short amount of time during which to make the measurement. Hydraulic modeling results formed the foundation for developing stage-discharge relations for high flows (the upper end of rating curves). We principally used HEC-RAS for hydraulic analyses, but TELEMAC-2D was used to examine hydraulic properties of the largest floods, following procedures similar to those employed for urban stream gages in Baltimore, Maryland [*Smith et al*., 2005a; *Lindner and Miller*, 2012]. Direct discharge measurements generally determine the lower end of the rating curves. The temporal resolution of discharge time series derived from stage measurements is 1 min.

In addition to the stream gaging stations, we deployed rain gages and a Joss-Waldvogel disdrometer in Harry's Brook (Figure 1a). The Joss-Waldvogel disdrometer was deployed for the 2006 observing period (the entire year). Disdrometer measurements provide full raindrop size distribution data from which rainfall rate time series can be computed at 1 min time intervals [*Smith et al*., 2009]. We setup rain gauges over two measurement sites (see Figure 1a for locations), and one of the two sites was collocated with the disdrometer. At each of the two measurement sites, two wedge-type accumulation rain gages were deployed. Observations were made manually for all storm events during the observing period of 2005–2006 (February 2005–December 2006). There was generally good agreement between the two gages at each measurement site. Accumulated rainfall of each storm event measured by the two gauges agrees well with the collocated disdrometer observations.

We computed rainfall rate fields at 1 km horizontal resolution and 15 min time interval using the Hydro-NEXRAD algorithm [*Krajewski et al*., 2011] which provide estimates of rainfall rate from volume scan reflectivity observations from the WSR-88D radar (the KDIX radar at Mount Holly, New Jersey, about 36 km to the south of Harry's Brook watershed; the elevation of the radar tower is 60 m above sea level). A constant "bias correction" was applied to the radar rainfall time series so that they matched the mean storm total rainfall from rain gage and disdrometer observations. This approach corresponds to a local version of the bias-correction algorithms commonly used for radar rainfall estimation [see also *Smith et al*., 2002]. The sample bias for a storm is computed as the ratio of the mean storm total rainfall at rain gage stations to the mean storm total rainfall from radar at rain gage locations (see *Villarini and Krajewski* [2010], *Smith et al*. [2013], *Wright et al*. [2013], and *Yang et al*. [2013] for more details about the bias-correction scheme).

Disdrometer, rain gages, and radar observations were used to derive rainfall fields for storm events in Harry's Brook and Simon Run during the 2 year observing period. Radar rainfall estimates were used for both Harry's Brook and Simon Run subwatershed to derive basin-averaged rainfall rate during the 2005 period, while higher-resolution rainfall rate from the disdrometer was used to analyze rainfall-runoff relationships during the 2006 period for both Harry's Brook and Simon Run. Table 1 summarizes three key variables that characterize storms that produced flash floods over Harry's Brook during 2005–2006 (see *Yang et al*. [2016] for details). All storms that occurred over Harry's Brook also passed over Simon Run. The spatial coverage of the two subwatersheds (approx. 1 km × 2 km, see Figure 1a) is approximate an order of magnitude smaller than the scale of a single storm element (i.e., a contiguous region of radar reflectivity values exceeding 40 dBZ and the total volume is greater than 50 km^3, same as below). Due to close proximity and favorable orientation of storm elements, most storms arrived at Harry's Brook and Simon Run at the same time. Rapid motion of storm elements (parallel to the connecting line of two subwatershed centers) diminishes the temporal shift of rainfall series between the two subwatersheds within 2 min (i.e., distance between two subwatersheds centers divided by mean storm speed).

Table 2. Statistics of GSSHA Model Validation for Selected 2006 Events Over Harry's Brook Subwatershed[a]

No.	Time (MM/DD-HH)	Peak Discharge ($m^3 s^{-1}$)	Response Time (min)	NSE	Timing Difference (min)	Absolute Peak Difference ($m^3 s^{-1}$)	Relative Peak Difference (%)
1	07/13-02	5.3	18	0.83	0	−0.55	−10.4
2	07/22-00	11.3	21	0.89	5	−1.60	−14.2
3	07/22-20	29.5	17	0.85	0	−13.04	−44.2
4	07/21-20	1.1	24	0.83	3	0.10	9.1
5	07/22-19	3.8	18	0.92	1	−0.75	−19.7
6	06/03-00	12.2	16	0.84	0	−3.95	−32.4
7	06/03-03	9.8	32	0.93	−1	−1.81	−18.5
8	06/03-16	3.9	22	0.94	−1	−0.52	−13.3
9	06/08-23	3.1	21	0.95	3	0.29	9.4
10	06/14-23	4.5	21	0.76	2	0.68	15.1
11	06/23-22	2.7	21	0.68	−1	0.58	21.5
12	06/24-10	2.6	20	0.87	2	−0.54	−20.8
13	06/24-22	1.3	26	0.89	4	−0.17	−13.1
14	05/16-00	2.8	23	0.81	1	−0.29	−10.4

[a]Response time is defined as the temporal lag between the centroids of hyetograph and hydrograph for each storm event.

3. Methodology

3.1. GSSHA Setup and Model Validation

The Gridded Surface Subsurface Hydrologic Analysis (GSSHA) model [*Downer and Ogden*, 2004] is a gridded, distributed, and physically based hydrologic model. The GSSHA model has been used successfully in urban flood studies over a variety of settings, such as Dead Run watershed in Maryland [*Ogden et al*., 2011; *Smith et al*., 2015], Atlanta, Georgia [*Wright et al*., 2014], and Austin, Texas [*Sharif et al*., 2010]. The structure of the model used in this study includes a 2-D overland flow representation, 1-D hydraulic routing of streamflow in the drainage systems, and grid-based infiltration routines. Previous studies found that the GSSHA model can adequately capture urban flood responses without "significant calibration" [*Sharif et al*., 2010].

We implemented the GSSHA model over the 1.1 km^2 Harry's Brook subwatershed. The model was created with 90 m resolution grids. The model elevation grid was created based on 1/3 arc sec (about 10 m) National Elevation Dataset (available at http://nationalmap.gov/) for watershed delineation and stream location. We used the diffusive wave equations for the simulation of overland flow routing. The land-use (National Land Cover Dataset of 2011, available at http://www.mrlc.gov/)-based Manning's roughness coefficients were directly adopted from suggested values in the literature [see *Kalyanapu et al*., 2009, Table 2]. Infiltration was represented using the Green-Ampt model with moisture redistribution [*Ogden and Saghafian*, 1997]. The Soil Survey Geographic Database (SSURGO, available at http://websoilsurvey.nrcs.usda.gov/) was used for soil data in the model, and in most cases, a compacted soil layer is present in the conductivity values. Soil parameters related to infiltration processes were adopted from previous studies [*Rawls et al*., 1982; *Rawls and Brakensiek*, 1985], with the exception of saturated hydraulic conductivity. Saturated hydraulic conductivity values were taken from the SSURGO database as the average of the given range for that soil type, and were further adjusted based on comparisons of modeled and observed streamflow volume for three storm events, to ensure best partition of rainfall into runoff and infiltration [similarly see *Smith et al*., 2015].

Channel and storm drainage networks play an important role as these constitute one of the principal hydraulic transport systems in urban watersheds [*Smith et al*., 2005b; *Meierdiercks et al*., 2010; *Miller et al*., 2014]. There are no surface stream channels in the Harry's Brook subwatershed (Figure 1). We added storm pipes into the model manually to represent the plan form of the storm drainage network. Routing of 1-D flow in storm pipes is based on diffusive wave equations. Detailed information on pipe elevation was not available, so we assumed a constant slope for each section of the pipes. Constant slopes of the pipes were derived from the ground elevation difference from the furthest pipe end to the connection node (i.e., intersection of two pipes) divided by the length of pipe path from connection node to pipe end. Cross sections for all the pipes were represented by a rounded semicircle bottom and walls reaching up vertically, with no capacity restrictions of the pipes in the model (see *Smith et al*. [2015] for similar approaches). The manholes/inlets were never witnessed to overtop in this watershed during the observing period of 2005–2006 (two of the coauthors lived near the center of the watershed). The model results were also spot checked to

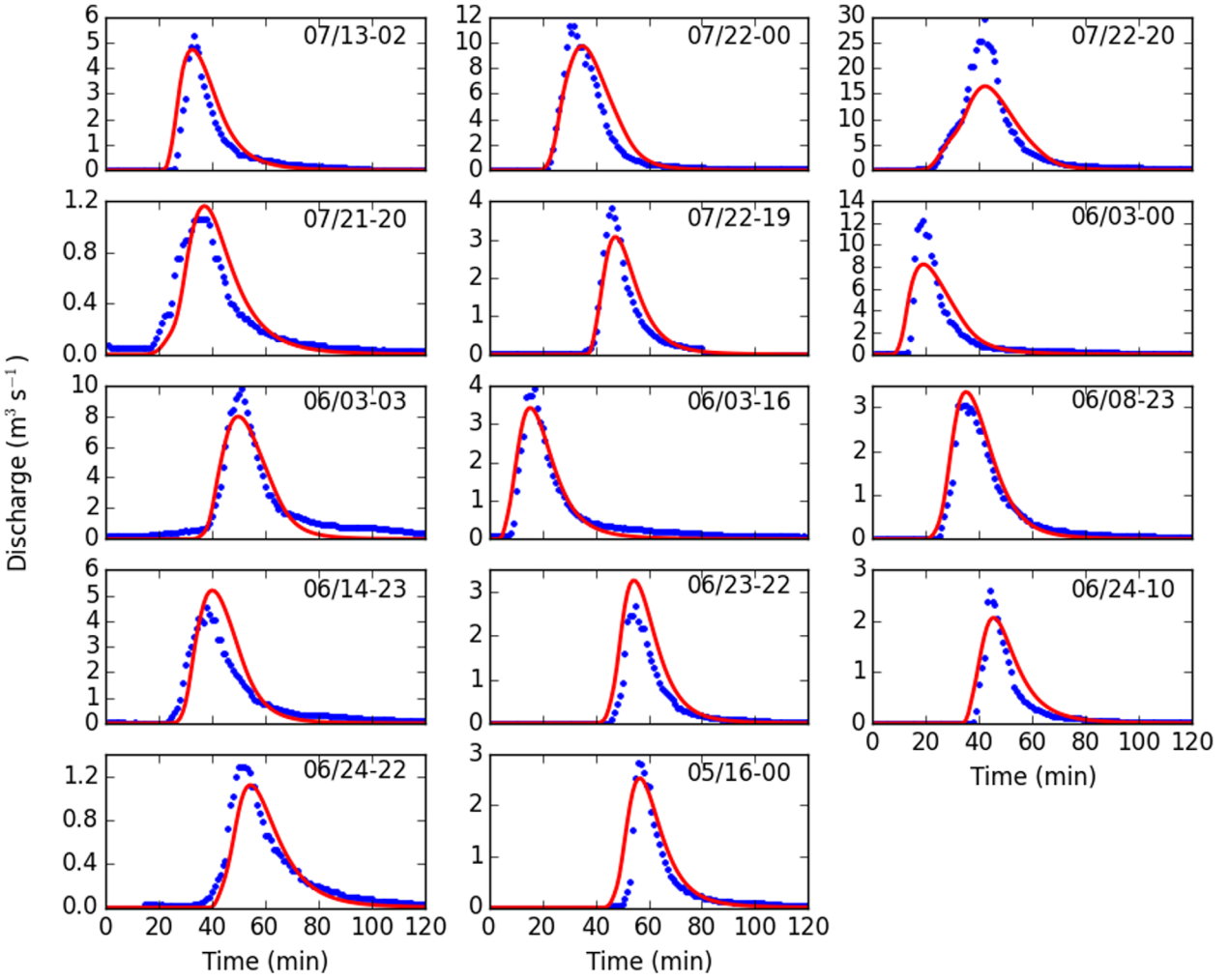

Figure 2. Model verification for selected 2006 events over Harry's Brook subwatershed: simulated (red solid line, in m^3 s^{-1}) and measured hydrographs (blue dots, in m^3 s^{-1}). The *x* axis represents time (in minute) since the beginning of model run. See also Table 2 for statistics about the performance of the model.

ensure that pipes were not over topping. The diameter of the pipes (or diameter of the circle) was 1 m, and Manning's roughness coefficients were assigned a value of 0.02 for all storm pipes in the model [*Chow*, 1959].

The GSSHA model was calibrated and verified for 14 selected events (with unit flood peak discharge exceeding 1 m^3 s^{-1} km^{-2}) over the Harry's Brook subwatershed during the observing period of 2006 (also see *Yang et al*. [2016] for more details about storm properties of the selected events). The rainfall input for the model is based on 1 min rain rate from the Joss-Waldvogel disdrometer, and is distributed uniformly over the entire subwatershed. Like the disdrometer rainfall input, the temporal resolution of the model simulations is 1 min. Soil moisture observations were not available in the watershed during the observing period of 2006. Soil moisture was set approximately to half of field capacity for every storm event, and we adjusted the values to minimize the sum of errors between simulated and "observed" hydrographs for each of the 14 selected events (as listed in Table 2).

The simulated hydrographs at the outlet of the model (located at the downstream end of the storm drain network) were compared to the observed discharge time series at 1 min resolution. Comparisons between simulated and "observed" hydrographs are shown in Figure 2, with detailed statistics of the model performance summarized in Table 2. The model accurately captures the shape and timing of the hydrographs. The Nash Sutcliffe Efficiency coefficients [*Nash and Sutcliffe*, 1970] range from 0.68 to 0.95, with a median value of 0.86 for all the 14 selected events. In terms of peak timing, most of the simulated peaks deviate within

±15% of mean response time (on the order of 20 min, see Table 2 for details). The only exception is 00 UTC 22 July (Event No. 2 in Table 2), for which the simulated flood peak is 5 min later than the observed peak (about 24% deviation of response time). The model reproduced the exact flood peak timing for the two most extreme events (22 July 20 UTC 2006 and 3 June 03 UTC 2006, Table 2). The simulated flood peak magnitudes do not agree with observations as well as the peak timing, especially for some of the most extreme events. For instance, the simulated flood peak magnitude for the 22 July event is underestimated by 40%. The differences in flood peak magnitudes could be partially attributed to errors in the rainfall field (as will be discussed in section 3.3) and to streamflow measurement errors tied to stage-discharge rating curves [*Potter and Walker*, 1981, 1985]. Biases in the simulated hydrologic response may also be attributable to features that were poorly represented or parameterized in the model [*Del Giudice et al*., 2015]. For instance, the simplified representations of pipes in the model might increase the capacity of pipe flows, while limited representation of complete storm drainage network in the model might underestimate the capacity of pipe flows; the compactness of urban soils is another source of uncertainty that could bias simulation of the infiltration process in the model.

Despite all these uncertainties, the GSSHA model successfully reproduced the correct ranks of flood events (the 22 July event maintains the largest flood peak over all simulated events). Overall, we were able to obtain reasonable hydrologic response to storm events that produced flash flooding with this physically based, minimally calibrated model over Harry's Brook subwatershed.

3.2. Numerical Experiments

Numerical experiments based on the calibrated GSSHA model were designed and implemented, with the principal objective of analyzing the impacts of rainfall variability (both in time and space) on hydrologic response for selected storm events (as listed in Table 2). Numerical simulations provide flexibility in analyzing "hypothetical" rainfall scenarios for each storm event, which is beyond the capability of observations alone. Details of rainfall scenarios are described below.

3.2.1. Temporal Rainfall Variability

Scenarios of temporal rainfall variability were generated by aggregating the 1 min rainfall input at different time intervals. We used a large set of aggregation time intervals ranging from 1 to 120 min (i.e., 1, 5, 10, 15, 20, 25, and 30 min), and subselected multiple critical time intervals (i.e., 3, 5, 10, 30, and 60 min) for further analyses. These critical time intervals were also recommended in previous studies [e.g., *Berne et al*., 2004; *Einfalt et al*., 2004; *Ochoa-Rodriguez et al*., 2015]. Model configurations and initial conditions were all kept the same for simulating each storm event.

Two key metrics were used to quantify the impact of coarsening temporal resolutions of rainfall input on flood response. The metrics focus on variations in both flood peak magnitude (RE_t) and peaking timing (ΔT_t), and take the forms:

$$RE_t = (Qmax_{1-\min} - Qmax_{t-\min})/Qmax_{1-\min} \quad (1)$$

$$\Delta T_t = T(Qmax)_{t-\min} - T(Qmax)_{1-\min} \quad (2)$$

where RE_t is the relative change in flood peak magnitude ($Qmax_{t-\min}$) corresponding to different averaging time intervals (e.g., 3, 5, and 10 min) of rainfall input, in relation to the 1 min rainfall input from the disdrometer. ΔT_t is the relative difference in flood peak timing.

3.2.2. Spatial Rainfall Variability

The GSSHA model was calibrated based on the 1 min rainfall rate observations from the disdrometer, which implicitly assumes rainfall was uniformly distributed over all model grids (Figure 3a). The uniform assumption deviates from reality, but observations are not available to further resolve spatial rainfall variability. The spatial resolution of conventional WSR-88D radar reflectivity fields (approximately 1 km) is not helpful in resolving finer-scale rainfall variability over Harry's Brook (1.1 km^2). Accurate representations of spatial rainfall variability call for rainfall fields with higher spatial resolutions (as provided by, e.g., X-band Radar). In this study, we investigate the sensitivity of storm event hydrologic response to spatial rainfall variability by designing "hypothetical" rainfall scenarios representing contrasting spatial patterns of rainfall. Three contrasting spatial patterns of rainfall (in addition to the "Uniform" rainfall scenario) were designed (Figures 3a–3d). We computed flow distance $d(x)$ for point x within the watershed to the outlet of watershed. The maximum flow distance for Harry's Brook is about 1.8 km. Rainfall input $r(x,t)$ over each point x is:

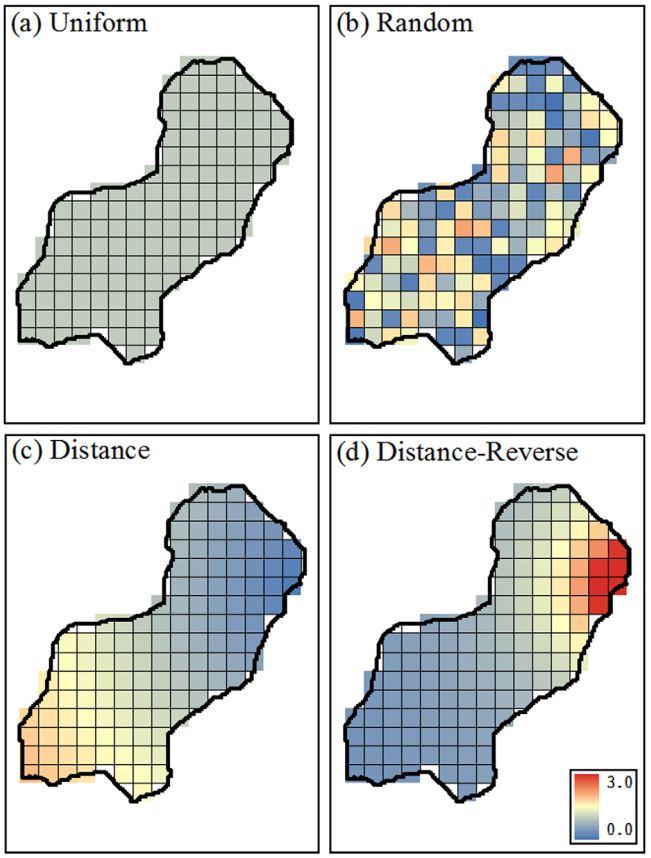

Figure 3. Weighting factors for four contrasting spatial rainfall patterns: (a) uniform, (b) random, (c) distance, and (d) distance-reverse. Shaded colors represent values of weighting factor $A\omega(x)$. Black line outlines the boundary of the watershed.

$$r(x,t)=\omega(x)R(t)A \tag{3}$$

Where A is the total area of the watershed, $R(t)$ is the 1 min rainfall rate from the disdrometer, $\omega(x)$ is the weighting factor, and have various expressions for different scenarios:

$$\text{Uniform}: \omega(x)=1/A \tag{4}$$

$$\text{"Random"}: \omega(x)=rand(x)/\int_A rand(x)dx \tag{5}$$

$$\text{"Distance"}: \omega(x)=d(x)/\int_A d(x)dx \tag{6}$$

$$\text{"Distance}-\text{Reverse"}: \omega(x)=[d(x)]^{-1}/\int_A [d(x)]^{-1}dx \tag{7}$$

where $rand(x)$ represents any random number between 0 and 1. The weighting factor is a function of location x, and is invariant with time. Spatial patterns representing rainfall variability are never exhaustive (see e.g., *Gires et al.* [2012] and *Paschalis et al.* [2014] for approaches to generate spatial rainfall patterns). In this study, we only present "end-member" scenarios (in terms of flood response) to represent spatial rainfall distribution over Harry's Brook. For instance, in the "Distance" scenario (Figure 3c), rainfall is assumed to concentrate in the upper region of the subwatershed, while rainfall is concentrated over the downstream region close to the outlet of the watershed in the "Distance-Reverse" scenario (Figure 3d). We set five different realizations for the "Random" scenario for each storm event. Model output from five different random realizations exhibited negligible variations. The averaged results from the five realizations are presented below to represent output of the "Random" scenario for each storm event. Rainfall input (1 min from the disdrometer), including both total accumulation and rain rate at each time step, is unchanged among different scenarios for each storm event.

Two key metrics were used to quantify the impact of spatial rainfall variability on flood response. The metrics focus on variations in both flood peak magnitude (RE_s) and timing (ΔT_s), and take the forms:

$$RE_s=(Qmax_{uniform}-Qmax_s)/Qmax_{uniform} \tag{8}$$

$$\Delta T_s=T(Qmax)_s-T(Qmax)_{uniform} \tag{9}$$

where RE_s is the relative change in flood peak magnitude ($Qmax_s$) corresponding to one of the three designed spatial rainfall scenarios (Random, Distance, and Distance-Reverse), relative to the "Uniform" scenario. ΔT_t is the relative difference in flood peak timing.

In addition to rainfall variability, numerical experiments based on GSSHA were designed to investigate sensitivity of flood response to antecedent soil moisture for specific events. We examine changes in both flood peak magnitudes and total runoff by setting up values that represent different initial conditions of soil moisture. These values range from 0.1 (the approximate wilting point, in volumetric fraction) to 0.5 (the approximate soil porosity, in volumetric fraction), with an interval of 0.1.

Table 3. Summary of the Hydrometeorological Variables for the 10 Biggest Flood Events in the Harry's Brook Subwatershed During the 2 Year Observing Period[a]

No.	Date (mm/dd/yy)	Peak Discharge ($m^3 s^{-1}$)	Rainfall (mm)	Runoff (mm)	Runoff Ratio	Max 1-Min Rain (mm h^{-1})	Max 15-Min Rain (mm h^{-1})	Max 30-Min Rain (mm h^{-1})
1	07/22/06	29.5	36.8	29.8	0.81	120	78	57
2	06/29/05	19.6	24.0	16.4	0.69	78	55	35
3	10/12/05	17.4	102.3	106.6	1.04	69	61	52
4	06/03/06	12.2	15.3	7.8	0.51	115	51	28
5	10/05/06	11.3	26.8	12.9	0.48	123	66	46
6	07/22/06*	11.3	18.3	8.5	0.46	88	61	37
7	10/09/05	11.0	101.0	80.4	0.80	62	50	38
8	07/02/05	10.4	15.0	7.4	0.49	93	50	29
9	06/03/06**	9.8	21.6	9.6	0.44	81	49	29
10	08/15/05	8.6	18.6	7.7	0.41	66	37	24

[a]The 22 July event in 2006 denoted with a star (for detailed information see Table 4, No.8) is a previous storm of the 22 July 2006 event that ranked No.1 in the table. The 3 June 2006 event marked with two stars (also see Table 4 No.7) is an event that happened after the storm that ranked No.4 in the table below. (Note: rainfall data for 2005 events are based on radar and for 2006 events are based on disdrometer, same as below).

4. Results and Discussion

In section 4.1, we examine rainfall-runoff relationships over Harry's Brook and Simon Run subwatersheds and highlight key factors (e.g., detention ponds, storm drainage network, depression storage, and antecedent soil moisture) that characterize hydrologic contrasts between the two subwatersheds. In the following two subsections, we investigate how rainfall variability in both time and space together with watershed characteristics determines storm event hydrologic response over Harry's Brook and Simon Run.

4.1. Rainfall-Runoff Relationships

There were 57 flood peaks in Harry's Brook exceeding 1 $m^3 s^{-1}$ during the 2 year observation period and 48 events with a unit discharge (i.e., flood peak discharge divided by drainage area) exceeding 1 $m^3 s^{-1} km^{-2}$, placing Harry's Brook among the "flashiest" watersheds in the U.S. [*Smith and Smith*, 2015]. Flood events are concentrated during the warm season; warm-season thunderstorms are the main agents for flash flooding in Harry's Brook, as in urban watersheds for much of the U.S. east of the Rocky Mountains [*Smith et al*., 2005a; *Ntelekos et al*., 2007; *Smith and Smith*, 2015; *Yang et al*., 2016; *Yeung et al*., 2015]. Ten events in Harry's Brook had values of peak discharge exceeding 8.6 $m^3 s^{-1}$ (unit discharge of 7.8 $m^3 s^{-1} km^{-2}$, see Table 3). Seven out of 10 occurred during the period from June to August and 3 occurred in October (Table 3).

As illustrated in Figures 4 and 5, peak discharge in Harry's Brook is strongly dependent on rainfall rate variability at 1–30 min time scales. Figure 4 presents scatterplots of maximum 5, 15, and 30 min rainfall rate and peak discharge for the 14 selected 2006 flood events in Harry's Brook. We use observations from the 2006 observing period because high-quality rainfall rate observations from disdrometer are available at 1 min time resolution. The correlation between maximum rain rate and peak discharge is 0.87 at a 5 min time scale, 0.94 at a 15 min time scale, and 0.92 at a 30 min time scale (Figure 5). The averaging time that produced the largest correlation between maximum x min rain rate and peak discharge in Harry's Brook is 13 min (Figure 5). Correlation increases from 0.70 at the 1 min time scale to 0.95 at 13 min time scale and decays gradually to 0.88 at 60 min time scale.

The storm event runoff ratios (i.e., the proportion of rainfall that becomes runoff) range from less than 0.1 to more than 0.8 (Figure 6) for the 2006 storm events in Harry's Brook. The striking variability in runoff ratio is linked to rainfall properties, antecedent storage, and heterogeneities of land surface processes, as described below. A quadratic representation of runoff as a function of storm total rain (Figure 6), characterizes the increase in runoff ratio with total rainfall. The nonlinear dependence between rainfall and runoff, characterized by a small rate of change at lower rainfall totals and a much larger rate of change at higher rainfall totals, is an important feature of flood hydrology for Harry's Brook. Similar features were reported for Dead Run at Franklintown, a 14.3 km^2 urban watershed in the Baltimore Metropolitan region [*Smith et al*., 2005b]. The increase in runoff ratio with total rainfall suggests that there are capacity constraints on storm event water balance imposed by both storage processes over pervious surfaces and depression storage over impervious surfaces in Harry's Brook. Previous studies found that total runoff was mainly contributed

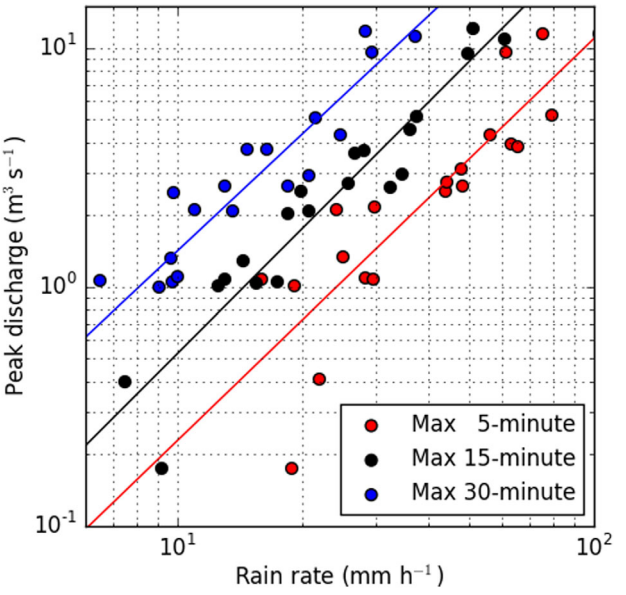

Figure 4. Relationship between flood peak discharge and maximum value of rainfall rates over 5 min (red dots), 15 min (black dots), and 30 min (blue dots) time averaging intervals for Harry's Brook subwatershed based on all the events during the 2006 observing period.

from impervious surfaces over the watersheds for small rainfall events, while pervious surfaces begin to contribute runoff for relatively larger rainfall events [*Terstriep and Stall*, 1969; *Miller and Viessman*, 1972].

A single pulse of rainfall is typically associated with passage of a convective storm element over Harry's Brook during a time period of approximately 1–30 min time scale [*Yang et al.*, 2016]. Flash floods are associated with organized convective systems in which multiple convective elements pass over a watershed [*Doswell et al.*, 1996]. Many of the 2005–2006 storms over the Harry's Brook subwatershed were characterized by multiple pulses of rainfall for which discharge rises and falls prior to the subsequent rainfall pulse (Table 4). The 22 July 2006 (Event No. 9 in Table 4) flood was associated with an approaching upper level trough and passage of a surface cold front. A cluster of convective cells developed in the warm sector east of the cold front, and moved toward Harry's Brook with storm speeds ranging at 30–50 km h^{-1} [*Yang et al.*, 2016]. Repeated passage of storm elements from the system played an important role in producing the largest flood peak in Harry's Brook. Multipulse flood response produced by storm elements embedded within organized convective systems is a key feature of flash flood hydrology over the Harry's Brook subwatershed.

We summarize water balance computations from multiple pulse storms in Table 4 with the objective of highlighting dependence of runoff properties on antecedent moisture state over the subwatershed. There is a general increase in runoff ratio for second pulse and third pulse events, but the more pronounced feature of these analyses is the dependence of runoff ratio on total rainfall (Figure 6). The three pulses of rain during the afternoon and evening of 22 July 2006 (Event No. 9 in Table 4) illustrate key features of the multipulse flood response to organized convective systems. A runoff ratio of 0.34 results from 8.3 mm of rainfall for the first rain pulse. The runoff ratio is 0.55 for the final pulse of rainfall, which was only 4.2 mm. Most importantly, the runoff ratio for the 28.5 mm of rainfall from the middle pulse was 0.95 and produced the record flood peak in Harrys Brook, a unit discharge of 26.8 $m^3 s^{-1} km^{-2}$. For Harry's Brook, rainfall of approximately 30 mm in 30 min produced runoff ratio close to 1 and a flood peak comparable to the largest unit discharge peaks from small urban watersheds in the U.S.

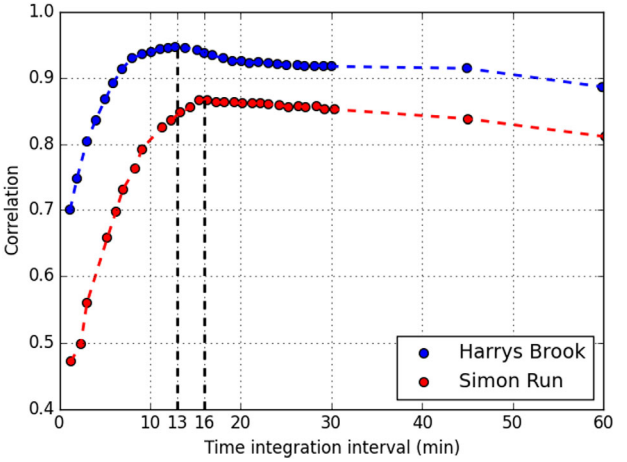

Figure 5. Correlation between peak discharge and maximum x min rainfall rate and time integration interval x (minute) for Harry's Brook (blue dots) and Simon Run (red circles) subwatershed, based on analyses carried out for events during the 2006 observing period. The maxima are highlighted with vertical dashed lines for both subwatersheds. Rain rates for both subwatersheds are based on the Joss-Waldvogel disdrometer (see Figure 1 for location).

The estimated peak discharge values in Simon Run for the ten largest flood peaks during the period of 2005–2006 are

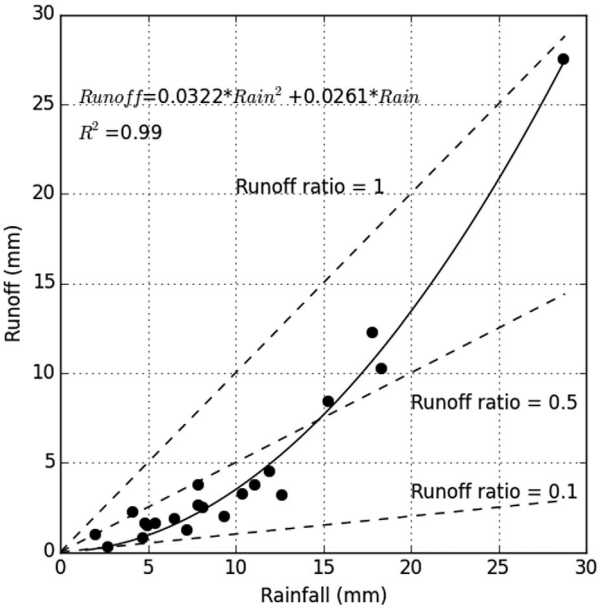

Figure 6. A scatterplot of event total rainfall (mm) and runoff (mm) for the Harry's Brook subwatershed based on events during the 2006 observing period. Black cure is the fitted line between runoff and rainfall, and the fitted function is listed in the figure. Dashed lines denote fixed runoff ratios.

markedly smaller than the ten largest values for Harry's Brook (Tables 3 and 5). The largest flood peak in Simon Run was 4.2 m^3 s^{-1} (unit discharge of 8.4 m^3 s^{-1} km^{-2}; Event No.1 in Table 5) for the 12 October 2005 storm which is ranked third for Harry's Brook (unit discharge of 15.8 m^3 s^{-1} km^{-2}; Event No. 3 in Table 3). The 22 July 2006 storm that produced the record flood peak at the Harry's Brook gaging station (unit discharge of 26.8 m^3 s^{-1} km^{-2}, see Table 3) ranked second at Simon run with a unit discharge peak of 6.6 m^3 s^{-1} km^{-2}. The reduction in peak discharge associated with storm water management for this record urban flood is roughly a factor of 4. The overlap among the list of top 10 flood events at the two sites is large, with the top 7 events at Simon Run (Table 5) all appearing in the top-10 list for Harry's Brook (Table 3).

The correlation between maximum rain rate (based on 1 min rainfall observation from the disdrometer) and peak discharge for Simon Run (Figure 5) is 0.65 at the 5 min time scale (0.87 in Harry's Brook), 0.86 at the 15 min time scale (0.94 in Harry's Brook) and 0.85 at the 30 min time scale (0.92 in Harry's Brook). The averaging time that produces the largest correlation between maximum x min rain rate and peak discharge for Simon Run is 16 min, 3 min longer than for Harry's Brook despite the fact that Simon Run is approximately half the drainage area. Correlation increases from 0.47 at a 1 min time scale to 0.87 at a 16 min time scale and decays gradually to 0.82 at 60 min time scale. Contrasting rainfall-runoff relationships between Harry's Brook and Simon Run highlight the role of watershed characteristics (e.g., detention ponds, efficient storm drainage network, depression storage, and antecedent soil moisture) in determining flood response.

Table 4. Summary of the Hydrometeorological Variables for Selected Multiple-Pulses Storm Events Over the Harry's Brook Subwatershed During the 2 Year Observing Period

No.	Date (mm/dd/yy)	Time (UTC)	Peak Discharge (m^3 s^{-1})	Rainfall (mm)	Runoff (mm)	Runoff Ratio	Max 15-Min Rain (mm h^{-1})	Time Between Peaks (h)
1	06/29/05	18:40	1.7	5.0	1.2	0.25	19	1.0
	06/29/05	19:38	19.6	19.0	15.2	0.80	55	
2	07/01/05	21:47	1.3	5.5	1.8	0.32	N/A	8.0
	07/01/05	05:46	10.4	15.0	7.4	0.49	50	
3	07/08/05	11:04	0.2	13.8	1.8	0.13	13	0.2
	07/08/05	15:32	1.3	25.4	5.1	0.20	26	
4	10/08/05	21:38	10.3	61.9	33.9	0.55	50	3.6
	10/08/05	01:22	11.0	39.1	46.5	1.19	30	
5	10/12/05	10:04	17.4	86.4	88.2	1.02	61	4.5
	10/12/05	14:32	6.1	15.9	18.4	1.16	14	
6	05/15/06	23:30	1.0	4.6	0.9	0.19	15	1.4
	05/15/06	00:56	2.8	6.5	1.8	0.28	26	
7	06/03/06	00:32	12.2	15.3	7.8	0.51	51	3.5
	06/03/06	03:59	9.8	21.6	9.6	0.44	49	13.0
	06/03/06	16:57	3.9	13.6	4.8	0.35	29	
8	07/21/06	20:00	0.2	2.7	0.2	0.08	9	0.9
	07/21/06	20:57	1.1	5.0	1.5	0.31	13	3.2
	07/22/06	00:11	11.3	18.3	8.5	0.46	61	
9	07/22/06	19:57	3.8	8.3	2.8	0.34	27	1.0
	07/22/06	20:55	29.5	28.5	27.0	0.95	78	2.1
	07/22/06	22:58	1.1	4.2	2.3	0.55	12	

Table 5. Summary of the Hydrometeorological Variables for the 10 Biggest Flood Events in Simon Run During the 2 Year Observing Period[a]

No.	Date (mm/dd/yy)	Peak Discharge ($m^3 s^{-1}$)	Rainfall (mm)	Runoff (mm)	Runoff Ratio	Max 1-Min Rain ($mm h^{-1}$)	Max 15-Min Rain ($mm h^{-1}$)	Max 30-Min Rain ($mm h^{-1}$)
1	10/12/05	4.2	102.3	97.4	0.95	69	61	52
2	07/22/06	3.3	36.8	7.1	0.19	120	78	57
3	10/09/05	3.1	101.0	63.1	0.62	62	50	38
4	07/22/06*	2.7	18.3	7.0	0.38	88	61	37
5	10/05/06	2.6	26.8	7.8	0.29	123	66	46
6	06/03/06	2.2	15.3	7.7	0.50	115	51	28
7	06/29/05	1.9	24.0	8.4	0.25	78	55	35
8	06/14/06	1.7	11.9	8.9	0.75	N/A	N/A	N/A
9	06/23/06	1.5	9.4	2.4	0.26	63	63	19
10	06/28/06	1.3	35.2	19.7	0.56	39	39	19

[a]The 22 July event in 2006 marked with a star is a previous storm of the 22 July 2006 event that ranked No. 2 in the table.

4.2. Temporal Rainfall Variability

The contrast in storm event hydrologic response between Harry's Brook and Simon Run is illustrated through time series of rainfall and discharge in the two subwatersheds to a pulse of extreme rain rates on 3 June 2006 (Figure 7). Rainfall rate rises sharply to a maximum 1 min rate of 115 mm h^{-1}; peak 15 min rainfall rate is 51 mm h^{-1}. Discharge time series are represented through unit discharge to facilitate comparison between Harry's Brook (1.1 km^2) and Simon Run (0.5 km^2). Despite its larger size, Harry's Brook peaks 7 min before Simon Run, and its unit discharge peak is more than twice as large as that from Simon Run. Analyses of 3-D radar reflectivity fields show that the spatial scale of storm elements responsible for the 3 June 2006 flood was approximately about 100 km^2, and the mean value of storm velocity was around 30 km h^{-1} [see *Yang et al.*, 2016, Figure 4]. The storm approaches Harry's Brook and Simon Run at the same time due to favorable spatial orientation of storm elements [see *Yang et al.*, 2016, Figure 6], which eliminates the temporal shift of rainfall series over two subwatersheds. We thus infer that the differences in temporal lag of flood peaks for the 3 June 2006 event is predominantly related to contrasting physical properties of the two subwatersheds.

The largest flood peak in Harry's Brook, as noted above, occurred on 22 July 2006. It was produced by an organized thunderstorm system characterized by large temporal and spatial variability of rainfall rate (see *Yang et al.* [2016] for analyses of storm structure and evolution). The peak rainfall rates at 1, 5, 15, and 30 min time interval were 120, 95, 78, and 57 mm h^{-1}, respectively. The event had a peak discharge of 29.5 $m^3 s^{-1}$ (unit discharge of 26.8 $m^3 s^{-1} km^{-2}$; Table 3). The 26.8 $m^3 s^{-1} km^{-2}$ unit discharge at a drainage area of 1.1 km^2 is comparable to the largest unit discharge flood peaks in the eastern U.S. [*Smith et al.*, 2005a; *Smith and Smith*, 2015]. The lag time between the 1 min maximum rain rate and peak discharge for the 22 July 2006 event was only 11 min.

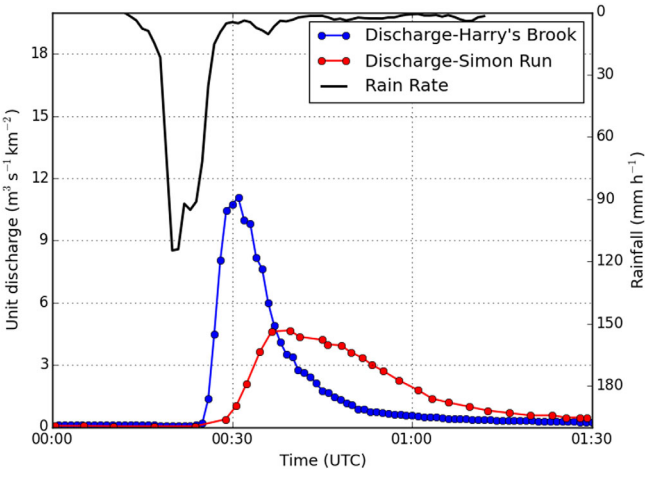

Figure 7. Time series of disdrometer rainfall rate (mm h^{-1}, black solid line) and unit discharge ($m^3 s^{-1} km^{-2}$) at both Harry's Brook (blue dotted line) and Simon Run (red dotted line) subwatersheds for the 3 June 2006 event during 0000 UTC-0130 UTC on 3 June 2006.

We carried out a series of numerical experiments using the GSSHA model (see section 3 for details) to examine the dependence of flood response on temporal rainfall variability. For the 22 July 2006 storm, the simulated peak discharge decreases from 16.9 $m^3 s^{-1}$ using disdrometer rainfall rates at 1 min time resolution to 4.7 $m^3 s^{-1}$ when rainfall rates are averaged to 120 min time interval (Figure 8a); We presented simulated peak discharge values for a broad range of averaging time intervals in Figure 8b. The simulated peak discharge generally decreases with the

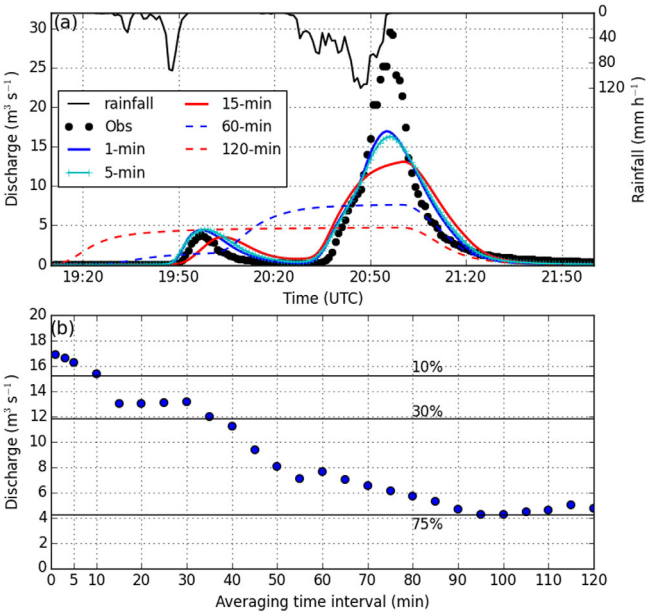

Figure 8. (a) Time series of disdrometer rainfall rate (black solid line, mm h^{-1}), observed hydrograph (black dots), and simulated discharge (m^3 s^{-1}) with rainfall rate averaged over 1, 5, 15, 60, and 120 min time interval, respectively, over Harry's Brook for the 22 July 2006 event; (b) scatterplot of simulated peak discharge for the 22 July 2006 event versus averaging time intervals ranging from 1 to 120 min. Horizontal lines represent difference in simulated peak discharge based on x min rainfall input relative to 1 min rainfall input ($RE_{x\,min}$) at levels of 10%, 30%, and 75%.

increasing averaging time interval. For time intervals larger than 30 min, the relative difference (RE_t) between simulated flood peak magnitude with rainfall rate at 1 and x min interval exceeds 30%, indicating significant reduction of simulated flood peak with the coarsening temporal resolution of rainfall input. The simulated peak discharge with rainfall rate at 3 and 5 min averaging interval are 16.5 and 16.3 m^3 s^{-1}, respectively, which are comparable to simulated flood peak of 16.9 m^3 s^{-1} with 1 min rainfall rate.

The reduction of flood peak due to coarsening temporal resolution of rainfall input is a common feature for all storm events over Harry's Brook (Figure 9). Simulations with rainfall input at 3 and 5 min averaging time intervals produced slight reduction (within 5%) of flood peak magnitude relative to 1 min rainfall input. The reduction rates exceed 50% with rainfall input at time averaging intervals larger than 30 min (Figure 9c). Coarsening simulations also delay the timing of simulated flood peak using rainfall input with larger averaging time intervals; there are only small variations in flood peak timing with smaller time intervals, e.g., 3 and 5 min (Figure 9d). The impacts of coarsening temporal resolution of rainfall input on simulated flood response (both in terms of flood peak magnitude and timing) are only weakly dependent on total rainfall (represented by maximum 60 min accumulated rainfall, Figures 9a and 9b). For the 1.1 km^2 scale of Harry's Brook, accurately resolving rainfall rate variability at 1–5 min time interval is critical for modeling flood peak response [e.g., *Berne et al.*, 2004; *Ochoa-Rodriguez et al.*, 2015].

In addition to temporal averaging of rainfall rates, the temporal distribution of rainfall pulses within a storm event plays an important role in flood response. The 21 July 2006 and 24 June 2006 events have comparable total rainfall amounts but contrasting temporal variability (Figures 10a and 10b). The 21 July 2006 event is characterized by a relatively uniform distribution of rainfall, while total rainfall is concentrated in a period of 10 min for the 24 June case, with peak rain rate over 60 mm h^{-1} (a factor of 3 larger than the 21 July rainfall peak). The corresponding flood response to the two rainfall series is quite different due to the distinct temporal distribution of rainfall forcing.

We present another set of comparable events (22 July 2006 and 3 June 2006, rank No. 1 and No. 4 in Table 3, respectively) in Figures 10c and 10d. Both cases have comparable maximum rain rates, but the main pulse on 22 July is preceded by a series of small pulses, while the 3 June is isolated from other rainfall pulses. Distinct flood peak magnitudes are observed due to temporal rainfall variability; the flood peak for 22 July is 3 times larger than the 3 June flood peak. We use numerical experiments with the GSSHA model to evaluate antecedent soil moisture impacts on flood response for the two events. Figure 11 highlights contrasting spatial patterns of antecedent soil moisture 15 min before flood peaks for both events. The entire subwatershed is almost saturated prior to the 22 July event, while the 3 June event exhibits a contrasting pattern, with only a small portion of saturated surface over the subwatershed. Accumulated rainfall within the 15 min interval (from the time of "soil moisture measurement" to time of flood peak) is 16.8 mm for 22 July and 12.5 mm for 3 June, respectively. Numerical experiments based on GSSHA for the 3 June event confirms the sensitivity of flood peaks and runoff ratio to antecedent soil moisture (see section 3 for more details about the experiments). The magnitude of flood peak for the 3 June case increases as a quadratic function of soil moisture (Figure 12). Flood peak magnitude is still much smaller than the 22 July case, even if we assigned a saturation

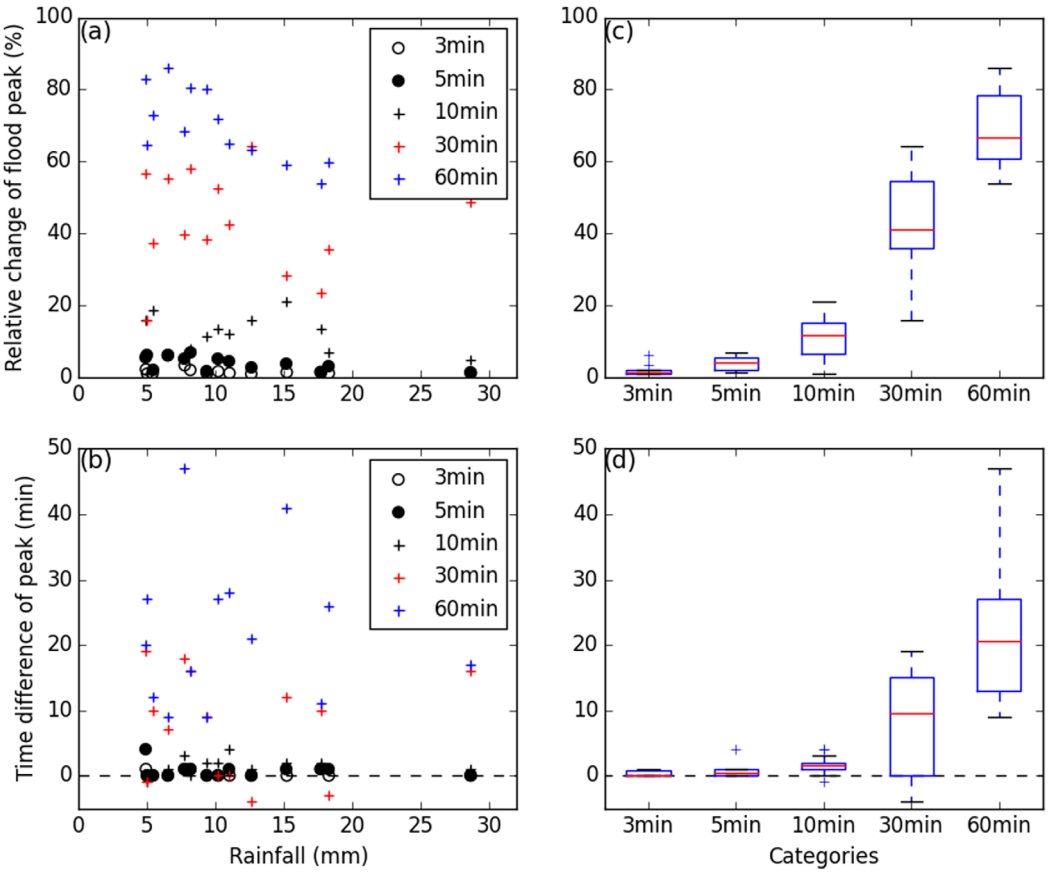

Figure 9. Numerical experiments based on GSSHA model for selected 2006 events (as listed in Table 1). (a, b) Relative difference between simulated flood peak magnitude and timing with rainfall rate at 1 and x min (x ranges among 3, 5, 10, 30, and 60) time interval. The events are indexed by total rainfall (accumulated rainfall within 60 min period). (c, d) The boxplots summarizing the differences as shown in Figures 9a and 9b. The box spans 0.25 and 0.75 percentiles, and the whiskers represent 0.1 and 0.9 percentiles. The red lines in the box represent median values.

value of antecedent soil moisture for the simulation. Combined analyses (based on Figures 11 and 12) indicate that total rainfall (which affects the depression storage in the surface or near-surface zones) is a more important factor in storm event water balance than conventional representations of antecedent soil moisture (also see Figure 6 for strong dependence of storm event runoff on total rainfall). Storm event hydrologic response to temporal rainfall variability is dictated by both antecedent soil moisture conditions and depression storage over impervious surfaces. However, water balance is strongly linked to peak rain rates at 1–30 min and weakly linked to antecedent soil moisture conditions (see *Smith et al.* [2013] for similar findings).

4.3. Spatial Rainfall Variability

We carried out a series of numerical experiments using the GSSHA model to examine the sensitivity of flood response to spatial variability of rainfall (see section 3 for details). Both flood peak magnitude and peak timing are sensitive to spatial variability of rainfall (Figure 13). Simulated flood peak magnitudes with random rainfall pattern are similar to the simulations with a uniform rainfall distribution (Figures 13a and 13c). Both "Distance" and "Distance-Reverse" rainfall patterns produce relatively larger flood peaks. The relative change of flood peak magnitude RE_s is around −15% (median values) for both "Distance" and "Distance-Reverse" scenarios. In addition, "Distance-Reverse" scenario reduced the time lags of flood peaks for all simulated events. This feature is expected since the main rainfall pulses are concentrated near the outlet which enables runoff to reach the outlet quickly (Figures 13b and 13d).

The Distance scenario, however, does not delay peak timing significantly compared to the "Uniform" rainfall scenario. The average difference in peak timing between "Distance" and "Uniform" rainfall scenario is between 0 and 2 min for all 14 events. The median value of peak timing differences between "Distance" and "Uniform" scenario is no more than 1 min larger than that between "Random" and "Uniform" scenario (Figure 13d). The

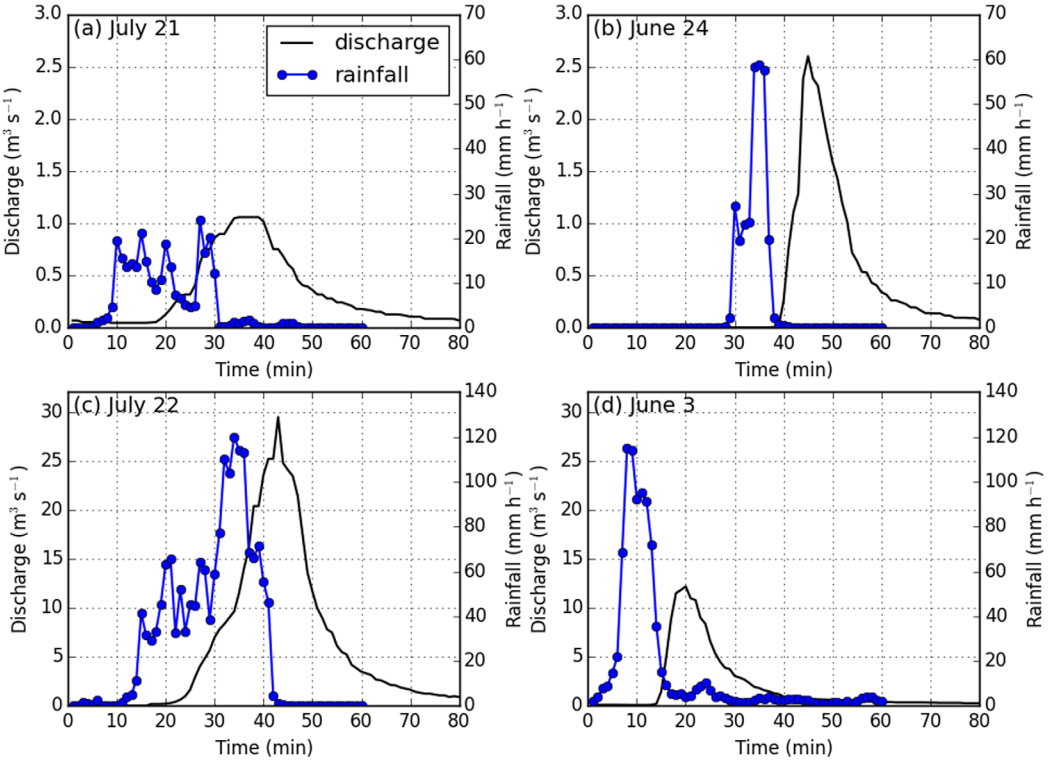

Figure 10. Time series of 1 min rainfall rate (mm h^{-1}) and discharge (m^3 s^{-1}) measured at the outlet of the Harry's Brook subwatershed for (a) 21 July 2006, (b) 24 June 2006, (c) 22 July 2006, and (d) 3 June 2006 event. Rain rate is measured by the Joss-Waldvogel disdrometer (see Figure 1 for location). *x* axis represents time (in minute) since the beginning of rainfall.

small difference in peak timing between "Distance" and "Uniform" scenario (also "Random" scenario) could be related to the high density of the storm drainage network in the upper portion of the subwatershed, which facilitates the rapid transport of runoff to the outlet [e.g., *Terstriep et al.*, 1976; *Graf*, 1977]. Well-designed and well-graded storm drainage systems (as is the case for Harry's Brook) are normally efficient channels with high water velocities that rapidly conduct runoff to the outlet [*Hollis*, 1975]. High density of storm drainage network in the upper portion of the subwatershed also contributes to increased flood peak magnitude in the Distance scenarios (Figure 13b) [e.g., *Hollis*, 1975; *Smith et al.*, 2002; *Ogden et al.*, 2011].

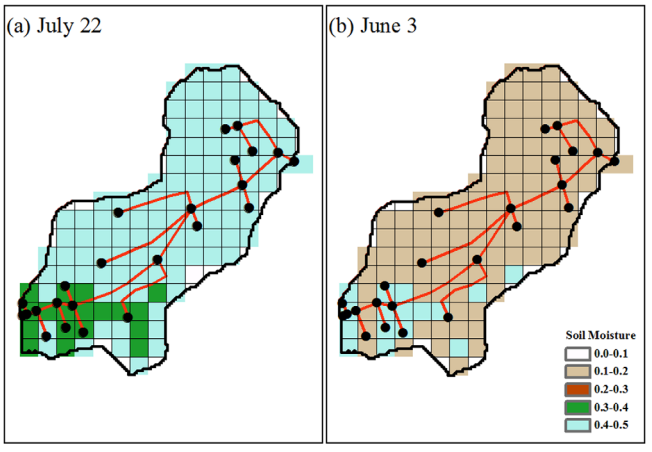

Figure 11. Spatial distribution of antecedent soil moisture (volumetric fraction, m^3 m^{-3}) in the Harry's Brook subwatershed for (a) 22 July 2006 and (b) 3 June 2006 case. The spatial maps shown here are instantaneous model output from the GSSHA model at 15 min before flood peaks for both cases. Storm drainage networks are shown in red solid lines and black dots. Black line represents watershed boundary.

Differences in both peak magnitudes and timing decrease dramatically with storm volume (represented by accumulated rainfall, Figures 13a and 13b), indicating that flood response to small rainfall events is more sensitive to spatial rainfall variability than large rainfall events. For the 22 July event (with the largest flood peak and total rainfall, indicated as the points on the far right of *x* axis in Figures 13a and 13b), flood peak magnitudes and timing do not vary much across different spatial rainfall scenarios. The lower sensitivity of flood response to spatial rainfall variability from intense storms relative to modest storms lies in the key runoff-generation and routing processes over Harry's Brook. For intense storms, the

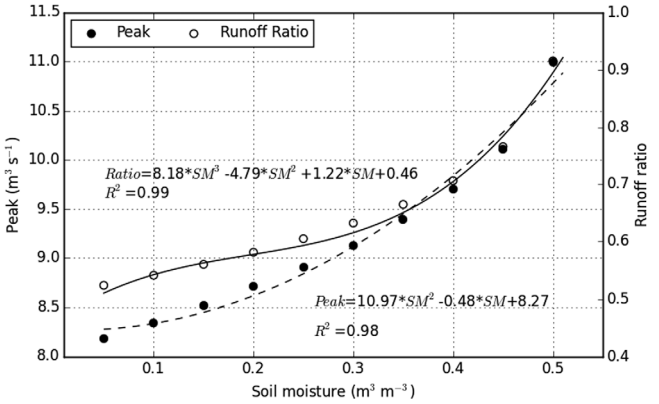

Figure 12. Sensitivity of flood peak (m^3 s^{-1}) and runoff ratio to antecedent soil moisture (averaged volumetric fraction over the entire subwatershed, m^3 m^{-3}) for the 3 June event over Harry's Brook subwatershed. The results are based on numerical experiments with GSSHA model. Regression and correlation analyses are also shown in the figure. We note that the upper limit of soil moisture is set to 0.5 (in volumetric fraction), corresponding to the porosity of soils over Harry's Brook subwatershed.

importance of depression storage in the surface or near-surface region (as discussed in previous sections) is greatly reduced (due to "saturation"). As a result, the entire watershed becomes "connected" with the storm drainage network, which enhances the efficiency of runoff transport to the outlet. For modest storms, flood response is dictated by the interplay of spatial rainfall variability and surface heterogeneities (e.g., spatial distribution of depression storage). A quantified influence of storage depression could be further investigated based on hydrodynamic modeling strategies with fine-scale resolutions and accurate representations of land surface properties in the model.

The relative importance of temporal and spatial rainfall variability in characterizing flood response could be discerned by the intensity of rainfall events over small urban watersheds (Figures 9 and 13). For extreme rainfall events, temporal rainfall variability (time-averaging and temporal distribution of rainfall pulses) plays

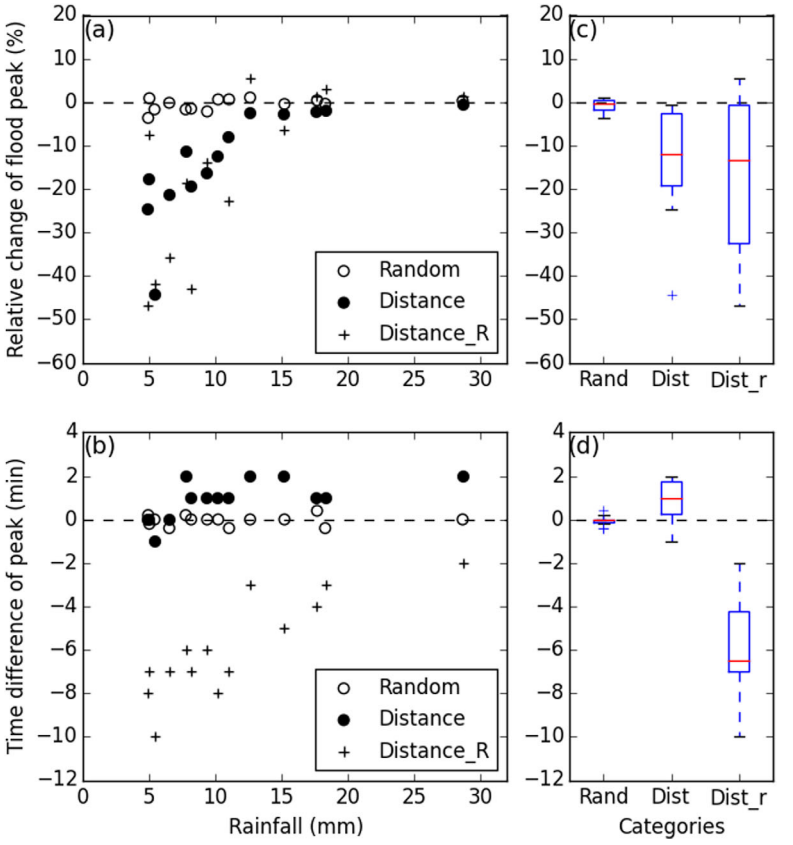

Figure 13. Numerical experiments based on GSSHA model for selected 2006 events (as listed in Table 2). (a, b) Relative differences in flood peak magnitude and timing with different spatial rainfall patterns, as compared to the uniform rainfall pattern. The events are indexed by total rainfall (accumulated rainfall within 60 min period, taking reference to the time of flood peak). (c, d) The boxplots summarizing the differences as shown in Figures 13a and 13b. The box spans 0.25 and 0.75 percentiles, and the whiskers represent 0.1 and 0.9 percentiles. The red lines in the box represent median values.

a relatively more important role than its spatial counterpart for the scenarios investigated in this paper in storm event hydrologic responses for small urban watersheds like Harry's Brook. Both spatial and temporal rainfall variability are critical in characterizing flood response to modest rainfall events.

5. Summary and Conclusions

Storm event hydrologic response over Harry's Brook and Simon Run is examined through analyses of rainfall and discharge observations as well as numerical simulations with the GSSHA model during a 2 year period (February 2005–October 2006). The principal conclusions of this study are summarized as follows:

1. For the Harry's Brook subwatershed at 1.1 km^2 drainage area, there were 57 flood peaks exceeding 1 $m^3\ s^{-1}$ during the 2004–2006 observing period. Ten events in Harry's Brook had peak discharge values exceeding 8.6 $m^3\ s^{-1}$ (unit discharge of 7.8 $m^3\ s^{-1}\ km^{-2}$), placing the watershed among the flashiest watershed in the U.S. [*Smith and Smith*, 2015]. Flood events are concentrated during the warm season, with seven out of ten occurred during the June-July-August period.
2. For Harry's Brook, correlation of peak discharge with maximum x min rain rate increases from 0.71 at 1 min to the 0.95 maximum at 13 min, and decreases to 0.88 at 60 min. For Simon Run at 0.5 km^2 drainage area, correlation of peak discharge with maximum x min rain rate increases from 0.47 at 1 min to the 0.87 maximum at 16 min, and decreases to 0.82 at 60 min. Spatial and temporal variability of rainfall rate, which are closely associated with structure and evolution of warm season thunderstorm systems, plays a key role in hydrologic response in urban watersheds.
3. Storm water management infrastructure plays a pronounced role in altering storm event hydrologic response. The Harry's Brook subwatershed was developed prior to storm water management regulations initiated during the 1970s and reflects "end-member" hydrologic response associated with rapid transmission of runoff through the storm drainage network. Simon Run was largely developed following implementation of storm water management regulations. Striking contrasts in hydrologic response to rain rate variability (see item 2 above and Figure 7) characterize the Simon Run and Harry's Brook observations during the 2005–2006 observing period, and place Harry's Brook among the flashiest watersheds in the U.S.
4. Variability in the storm event runoff ratio of Harry's Brook is large, ranging from less than 0.1 to more than 0.8 in the Harry's Brook subwatershed. Storm event runoff increases quadratically with storm total rainfall, with a much steeper rate of change for higher rainfall totals than for lower rainfall totals. Analyses suggest that storage processes in pervious portions of the watershed and depression over impervious portions of the watershed impose capacity constraints that control storm event water balance. Analyses of multipulse storm events (Table 4) and numerical experiments with GSSHA on sensitivity of flood response to antecedent soil moisture (Figures 11 and 12) provide only weak evidence of antecedent soil moisture controls of the storm event water balance. The quantitative impacts of antecedent soil moisture and depression storage on flood response, however, remain an important topic for future studies.
5. Numerical experiments based on the GSSHA model are used to evaluate the sensitivity of storm event flood responses to spatial and temporal variability of rainfall. Analyses on the 22 July 2006 event highlight the striking dependence of flood response on temporal variability of rainfall (Figures 8b and 10a). The modeled peak discharge decreases from 16.9 $m^3\ s^{-1}$ at 1 min time interval to 4.7 $m^3\ s^{-1}$ for an averaging time interval of 120 min. *Ochoa-Rodriguez et al*. [2015] found that the impact of temporal rainfall resolution decreases significantly when coarser temporal resolution estimates are generated through aggregation as opposed to sampling (e.g., sampling rainfall at desired time steps). Modeling analyses highlight the conditional sensitivity of flood response to spatial variability of rainfall, given the magnitude of 60 min accumulated rainfall. The impact of spatial rainfall variability on hydrologic response decreases as total rainfall accumulation increases. Sensitivity of hydrologic response to temporal rainfall variability does not clearly depend on storm intensity. For extreme rainfall events, temporal variability of rainfall plays a relatively more important role than its spatial counterpart in storm event hydrologic response over Harry's Brook. Resolving rainfall variability at fine temporal resolution (1–5 min) is thus a main concern in urban hydrology studies (see also e.g., *Ochoa-Rodriguez et al*. [2015] for similar conclusion). Higher resolution of rainfall fields at both temporal and spatial scales, is however desirable. *Gires et al*. [2012, 2014] and *Wang et al*. [2012] quantified the significant impacts of small-scale rainfall variability on simulated urban runoff. Recent studies explored the utility of approaches to interpolate operational

radar rainfall products (typically at 1 km/5–15 min resolution) onto finer temporal resolutions [e.g., *Thorndahl et al.*, 2014; *Nielsen et al.*, 2014; *Wang et al.*, 2015]. A recent operational rainfall product, Multi-Radar Multi-Sensor (MRMS) quantitive precipitation estimate at 1 km/2.5 min resolution [*Zhang et al.*, 2015] has potential application in urban hydrology studies.

Acknowledgments
We thank three anonymous reviewers and Susana Ochoa-Rodriguez for their useful comments and criticisms which helped to improve the manuscript substantially. We would like to extend our acknowledgements to Robert Kiser and the staff of Princeton Township for assistance in developing the Harry's Brook monitoring program. Data used in this study are archived at Princeton University and are available through the authors. The research was supported by the National Science Foundation (grants EEC-0540832, CBET-1058027, CBET-1444758, and AGS-1522492). L.Y. also confirms support by China Postdoctoral Science Foundation funded project (2015M570110).

References

Albrecht, J. C. (1974), Alterations in the hydrologic cycle induced by urbanization in northern New Castle county, Delaware: Magnitudes and projections, *Library Rep. DI-14-31-0001-3508, DI-14-31-0001-3808, OWRR-A-017-DEL, W74- 07729, OWRR-A-017-DEL(2)*, U.S. Environ. Prot. Agency, University of Delaware, Delaware.

Anderson, D. G. (1968), *Effects of urban development on floods in northern Virginia*, open file report, U.S. Geol. Surv., Washington, D. C.

Beighley, R. E. (2003), Adjusting measured peak discharges from an urbanizing watershed to reflect a stationary land use signal, *Water Resour. Res.*, *39*(4), 1093, doi:10.1029/2002WR001846.

Berne, A., G. Delrieu, J.-D. Creutin, and C. Obled (2004), Temporal and spatial resolution of rainfall measurements required for urban hydrology, *J. Hydrol.*, *299*(3-4), 166–179.

Bruni, G., R. Reinoso, N. C. van de Giesen, F. H. L. R. Clemens, and J. A. E. ten Veldhuis (2015), On the sensitivity of urban hydrodynamic modelling to rainfall spatial and temporal resolution, *Hydrol. Earth Syst. Sci.*, *19*(2), 691–709.

Chow, V. T. (1959), *Open Channel Hydraulics*, McGraw-Hill, N. Y.

Del Giudice, D., P. Reichert, V. Bareš, C. Albert, and J. Rieckermann (2015), Model bias and complexity-understanding the effects of structural deficits and input errors on runoff predictions, *Environ. Model. Software*, *64*, 205–214.

Doswell, C. A., H. E. Brooks, and R. A. Maddox (1996), Flash flood forecasting: An ingredients-based methodology, *Weather Forecasting*, *11*(4), 560–581.

Downer, C., and F. Ogden (2004), GSSHA: Model to simulate diverse stream flow producing processes, *J. Hydrol. Eng.*, *9*(3), 161–174.

Einfalt, T., K. Arnbjerg-Nielsen, C. Golz, N. E. Jensen, M. Quirmbach, G. Vaes, and B. Vieux (2004), Towards a roadmap for use of radar rainfall data in urban drainage, *J. Hydrol.*, *299*(3-4), 186–202.

Emmanuel, I., H. Andrieu, E. Leblois, and B. Flahaut (2012), Temporal and spatial variability of rainfall at the urban hydrological scale, *J. Hydrol.*, *430-431*, 162–172.

Farahmand, T., S. W. Fleming, and E. J. Quilty (2007), Detection and visualization of storm hydrograph changes under urbanization: An impulse response approach, *J. Environ. Manage.*, *85*(1), 93–100.

Gires, A., C. Onof, C. Maksimović, D. Schertzer, I. Tchiguirinskaia, and N. Simoes (2012), Quantifying the impact of small scale unmeasured rainfall variability on urban runoff through multifractal downscaling: A case study, *J. Hydrol.*, *442*, 117–128.

Gires, A., A. Giangola-Murzyn, J.-B. Abbes, I. Tchiguirinskaia, D. Schertzer, and S. Lovejoy (2014), Impacts of small scale rainfall variability in urban areas: A case study with 1D and 1D/2D hydrological models in a multifractal framework, *Urban Water J.*, *12*, 607–617.

Graf, W. L. (1977), Network characteristics in suburbanizing streams, *Water Resour. Res.*, *13*, 459–463, doi:10.1029/WR013i002p00459.

Hollis, G. E. (1975), Effect of urbanization on floods of different recurrence interval, *Water Resour. Res.*, *11*, 431–435.

Hundecha, Y., and A. Bárdossy (2004), Modeling of the effect of land use changes on the runoff generation of a river basin through parameter regionalization of a watershed model, *J. Hydrol.*, *292*(1-4), 281–295.

Kalyanapu, A. J., S. J. Burian, and T. N. Mcpherson (2009), Effect of land use-based surface roughness on hydrologic model output, *J. Spatial Hydrol.*, *9*(2), 51–71.

Konrad, C. P. (2003), Effects of urban development on floods, Fact Sheet 076-03, 4 pp., US Geological Survey, Reston, Va.

Konrad, C. P., and D. B. Booth (2002), Hydrologic trends associated with urban development for selected streams in the Puget Sound Basin, Western Washington, *U.S. Geol. Surv. Water Resour. Invest. Rep., 02-4040.*

Krajewski, W. F., et al. (2011), Towards better utilization of NEXRAD data in hydrology: An overview of Hydro-NEXRAD, *J. Hydroinf.*, *13*(2), 255–266.

Leopold, L. (1968), Hydrology for urban land planning-a guidebook on the hydrologic effects of urban land use, *Geol. Surv. Circ.*, *554*, 1–21.

Lindner, G. A, and A. J. Miller (2012), Numerical modeling of stage-discharge relationships in urban streams, *J. Hydrol. Eng.*, *17*(4), 590–596.

Meierdiercks, K. L., J. A. Smith, M. L. Baeck, and A. J. Miller (2010), Analyses of urban drainage network structure and its impact on hydrologic response, *J. Am. Water Resour. Assoc.*, *46*(5), 932–943.

Miller, C. R., and W. Viessman (1972), Runoff volumes from small urban watersheds, *Water Resour. Res.*, *8*, 429–434.

Miller, J. D., H. Kim, T. R. Kjeldsen, J. Packman, S. Grebby, and R. Dearden (2014), Assessing the impact of urbanization on storm runoff in a peri-urban catchment using historical change in impervious cover, *J. Hydrol.*, *515*, 59–70.

Nash, E., and V. Sutcliffe (1970), River flow forecasting through conceptual models part I-a discussion of principles, *J. Hydrol.*, *10*, 282–290.

Nielsen, J. E., S. Thorndahl, and M. R. Rasmussen (2014), A numerical method to generate high temporal resolution precipitation time series by combining weather radar measurements with a nowcast model, *Atmos. Res.*, *138*, 1–12.

Notaro, V., C. M. Fontanazza, G. Freni, and V. Puleo (2013), Impact of rainfall data resolution in time and space on the urban flooding evaluation, *Water Sci. Technol.*, *68*(9), 1984–1993.

Ntelekos, A. A., J. A. Smith, and W. F. Krajewski (2007), Climatological analyses of thunderstorms and flash floods in the Baltimore metropolitan region, *J. Hydrometeorol.*, *8*(1), 88–101.

Ochoa-Rodriguez, S., et al. (2015), Impact of spatial and temporal resolution of rainfall inputs on urban hydrodynamic modelling outputs: A multicatchment investigation, *J. Hydrol.*, *531*, 389–407.

Ogden, F. L., and B. Saghafian (1997), Green and Ampt infiltration with redistribution, *J. Irrig. Drain. Eng.*, *123*(5), 386–393.

Ogden, F. L., H. O. Sharif, S. U. S. Senarath, J. A. Smith, M. L. Baeck, and J. R. Richardson (2000), Hydrologic analysis of the Fort Collins, Colorado, flash flood of 1997, *J. Hydrol.*, *228*(1-2), 82–100.

Ogden, F. L., N. Raj Pradhan, C. W. Downer, and J. A. Zahner (2011), Relative importance of impervious area, drainage density, width function, and subsurface storm drainage on flood runoff from an urbanized catchment, *Water Resour. Res.*, *47*, 1-12.

Paschalis, A., S. Fatichi, P. Molnar, S. Rimkus, and P. Burlando (2014), On the effects of small scale space-time variability of rainfall on basin flood response, *J. Hydrol.*, *514*, 313–327.

Potter, W., and J. F. Walker (1981), A model of discontinuous measurement error and its effects on the probability distribution of flood discharge measuremen, *Water Resour. Res.*, *17*, 1505–1509.

Potter, K. W., and J. F. Walker (1985), An empirical study of flood measurement error, *Water Resour. Res.*, *21*, 403–406.

Rawls, W. J., and D. L. Brakensiek (1985), Prediction of soil water properties for hydraulic modeling, in *Proceedings of Symposium Watersed Management in the Eighties*, pp. 293–299, Am. Soc. of Civ. Eng., N. Y.
Rawls, W. J., D. L. Brakensiek, and K. E. Saxton (1982), Estimation of soil water properties, *Trans. ASAE*, *25*(5), 1316–1320 and 1328.
Sauer, V. B., W. O. Thomas, V. A. Stricker, and K. V. Wilson (1983), Flood characteristics of urban watersheds in the United States, U.S. Geol. Surv. Water Supp. Pap., 2207, 69 pp.
Segond, M. L., H. S. Wheater, and C. Onof (2007), The significance of spatial rainfall representation for flood runoff estimation: A numerical evaluation based on the Lee catchment, UK, *J. Hydrol.*, *347*, 116–131.
Schilling, W. (1991), Rainfall data for urban hydrology: What do we need?, *Atmos. Res.*, *27*, 5–21.
Sharif, H. O., A. A. Hassan, S. Bin-Shafique, H. Xie, and J. Zeitler (2010), Hydrologic modeling of an extreme flood in the guadalupe river in Texas, *J. Am. Water Resour. Assoc.*, *46*(5), 881–891.
Shuster, W. D., J. Bonta, H. Thurston, E. Warnemuende, and D. R. Smith (2005), Impacts of impervious surface on watershed hydrology: A review, *Urban Water J.*, *2*(4), 263–275.
Smith, B. K., and J. A. Smith (2015), The flashiest watersheds in the contiguous United States, *J. Hydrometeorol.*, *16*(6), 2365–2381, doi: 10.1175/JHM-D-14-0217.1.
Smith, B. K., J. A. Smith, M. L. Baeck, G. Villarini, and D. B. Wright (2013), Spectrum of storm event hydrologic response in urban watersheds, *Water Resour. Res.*, *49*, 2649–2663, doi:10.1002/wrcr.20223.
Smith, B. K., J. A. Smith, M. L. Baeck, and A. J. Miller (2015), Exploring storage and runoff generation processes for urban flooding through a physically based watershed model, *Water Resour. Res.*, *51*, 1552–1569, doi:10.1002/2014WR016085.
Smith, J. A., M. L. Baeck, J. E. Morrison, P. Sturdevant-Rees, D. F. Turner-Gillespie, and P. D. Bates (2002), The regional hydrology of extreme floods in an urbanizing drainage basin, *J. Hydrometeorol.*, *3*(3), 267–282.
Smith, J. A., A. J. Miller, M. L. Baeck, P. A. Nelson, G. T. Fisher, and K. L. Meierdiercks (2005a), Extraordinary flood response of a small urban watershed to short-duration convective rainfall, *J. Hydrometeorol.*, *6*(5), 599–617.
Smith, J. A., M. L. Baeck, K. L. Meierdiercks, P. A. Nelson, A. J. Miller, and E. J. Holland (2005b), Field studies of the storm event hydrologic response in an urbanizing watershed, *Water Resour. Res.*, *41*, W10413, doi:10.1029/2004WR003712.
Smith, J. A., E. Hui, M. Steiner, M. L. Baeck, W. F. Krajewski, and A. A. Ntelekos (2009), Variability of rainfall rate and raindrop size distributions in heavy rain, *Water Resour. Res.*, *45*, W04430, doi:10.1029/2008WR006840.
Terstriep, M. L., and J. B. Stall (1969), Urban runoff by the road research laboratory method, *J. Hydraul. Div.*, *95*(HY6), 1809–1834.
Terstriep, M. L., M. L. Voorhees, and G. M. Bender (1976), *Conventional Urbanization and Its Effect on Storm Runoff*, Ill. State Water Surv., Urbana, Ill.
Thorndahl, S., J. E. Nielsen, and M. R. Rasmussen (2014), Bias adjustment and advection interpolation of long-term high resolution radar rainfall series, *J. Hydrol.*, *508*, 214–226.
Villarini, G., and W. F. Krajewski (2010), Review of the different sources of uncertainty in single polarization radar-based estimates of rainfall, *Surv. Geophys.*, *31*(1), 107–129.
Wang, L.-P., C. Onof, S. Ochoa-Rodríguez, N. E. Simoes, and C. Maksimović (2012), On the propagation of rainfall bias and spatial variability through urban pluvial flood modelling, paper presented at 9th International Workshop on Precipitation in Urban Areas: Urban challenges in rainfall analysis, Saint Moritz, Switzerland, ETH Zurich - Swiss Federal Institute of Technology.
Wang, L.-P., S. Ochoa-Rodríguez, J. Van Assel, R. D. Pina, M. Pessemier, S. Kroll, P. Willems, and C. Onof (2015), Enhancement of radar rainfall estimates for urban hydrology through optical flow temporal interpolation and Bayesian gauge-based adjustment, *J. Hydrol.*, *531*, 408–426.
Wibben, H. C. (1976), Effects of urbanization on flood characteristics in Nashville-Davidson County, Tennessee, *U.S. Geol. Surv. Water Resour. Invest. report*, 76–121.
Wright, D. B., J. A. Smith, G. Villarini, and M. L. Baeck (2012), Hydroclimatology of flash flooding in Atlanta, *Water Resour. Res.*, *48*, W04524, doi:10.1029/2011WR011371.
Wright, D. B., J. A. Smith, G. Villarini, and M. L. Baeck (2013), Long-term high-resolution radar rainfall fields for urban hydrology, *J. Am. Water Resour. Assoc.*, *50*(3), 713–734.
Wright, D. B., J. A. Smith, and M. L. Baeck (2014), Flood frequency analysis using radar rainfall fields and stochastic storm transposition, *Water Resour. Res.*, 1592–1615, doi:10.1002/2013WR014224.
Yang, G., L. C. Bowling, K. A. Cherkauer, B. C. Pijanowski, and D. Niyogi (2010), Hydroclimatic response of watersheds to urban intensity: An observational and modeling-based analysis for the White River basin, Indiana, *J. Hydrometeorol.*, *11*(1), 122–138.
Yang, L., J. A. Smith, D. B. Wright, M. L. Baeck, G. Villarini, F. Tian, and H. Hu (2013), Urbanization and climate change: An examination of nonstationarities in urban flooding, *J. Hydrometeorol.*, *14*(6), 1791–1809.
Yang, L., F. Tian, and D. Niyogi (2015), A need to revisit hydrologic responses to urbanization by incorporating the feedback on spatial rainfall patterns, *Urban Clim.*, *12*, 128–140.
Yang, L., J. A. Smith, M. L. Baeck, D. Niyogi, and F. Tian (2016), Structure and evolution of flash flood producing storms in small urban watersheds, *J. Geophy. Res.*, *121*, 3139–3152, doi:10.1002/2015JD024478.
Yeung, J. K., J. A. Smith, M. L. Baeck, and G. Villarini (2015), Lagrangian analyses of rainfall structure and evolution for organized thunderstorm systems in the urban corridor of the northeastern US, *J. Hydrometeorol.*, *16*(4), 1575–1595.
Zhang, J., et al. (2015), Multi-Radar Multi-Sensor (MRMS) quantitative precipitation estimation: Initial operating capabilities, *Bull. Am. Meteorol. Soc.*, *97*(4), 621–638, doi:10.1175/BAMS-D-14-00174.1.
Zhang, Y., and W. Shuster (2014), Impacts of spatial distribution of impervious areas on runoff response of hillslope catchments: Simulation study, *J. Hydrol. Eng.*, *19*(6), 1089–1100.
Zhang, Y., and J. A. Smith (2003), Space-time variability of rainfall and extreme flood response in the Menomonee River Basin, Wisconsin, *J. Hydrometeorol.*, *4*(3), 506–517.